

# Quantum belief function<sup>★</sup>

Qianli Zhou<sup>a,b,1</sup>, Guojing Tian<sup>b</sup> and Yong Deng<sup>a,c,d,e,\*</sup>

<sup>a</sup>*Institute of Fundamental and Frontier Science, University of Electronic Science and Technology of China, Chengdu, 610054, China*

<sup>b</sup>*Institute of Computing Technology, Chinese Academy of Sciences, Beijing, China*

<sup>c</sup>*School of Education Shannxi Normal University, Xi'an, 710062, China*

<sup>d</sup>*School of Knowledge Science, Japan Advanced Institute of Science and Technology, Nomi, Ishikawa 923-1211, Japan*

<sup>e</sup>*Department of Management, Technology, and Economics, ETH Zurich, Zurich, 8093, Switzerland*

## ARTICLE INFO

### Keywords:

Dempster-Shafer evidence theory  
Quantum evidence theory  
Quantum circuit  
Quantum basic belief assignment  
Quantum belief function  
Evidence fidelity

## ABSTRACT

The belief function in Dempster Shafer evidence theory can express more information than the traditional Bayesian distribution. It is widely used in approximate reasoning, decision-making and information fusion. However, its power exponential explosion characteristics leads to the extremely high computational complexity when handling large amounts of elements in classic computers. In order to solve the problem, we encode the basic belief assignment (BBA) into quantum states, which makes each qubit correspond to control an element. Besides the high efficiency, this quantum expression is very conducive to measure the similarity between two BBAs, and the measuring quantum algorithm we come up with has exponential acceleration theoretically compared to the corresponding classical algorithm. In addition, we simulate our quantum version of BBA on Qiskit platform, which ensures the rationality of our algorithm experimentally. We believe our results will shed some light on utilizing the characteristic of quantum computation to handle belief function more conveniently.

## 1. Introduction

For a random variable with  $n$  basic events, the classical probability theory uses  $n$ -dimensional probability distribution to represent its uncertainty. However, in reality, we always cannot get an accurate probability distribution. In order to express information without complete probability distribution, Dempster (2008) and Shafer (1976) propose Dempster-Shafer evidence theory (DSET) based on the multi-valued mapping of basic events. They use  $2^n$  mass functions called basic belief assignment (BBA) to express the degree of support for  $n$  basic events. Therefore, BBA can express more uncertainty than the Bayesian distribution, which makes it widely applied in pattern recognition Denoeux (1994), multi-criteria decision-making Deng, Zheng, Su, Chan, Hu, Sadiq and Deng (2014) and medical diagnosis Zhou, Mo and Deng (2020). Although using high-dimensional distribution to express low-dimensional events can express more uncertainty of the events, there are still some unsolved problems in DSET. First, due to the incomplete mutual exclusion between focal elements, there is no conditional BBA expressed by mass function in DSET. Even though some scholars use belief function to describe conditional BBA Yaghlane, Smets and Mellouli (2002) Dezer, Tchamova and Han (2018), they still cannot utilize prior knowledge sufficiently in decision-making. Secondly, because BBA has not only the discord to express the conflict between events (elements), but the non-specificity to express the uncertainty of the distribution as well, how to measure the total uncertainty of BBA and inference the difference between BBAs are significant in decision-making. The fractal-based belief entropy we put forward in Zhou and Deng (2020) can basically solve the former problem, and Jousselme *et al.* Jousselme, Grenier and Bossé (2001) propose the distance of evidence to solve the latter problem. The biggest dilemma in DSET is power exponential explosion. BBA uses  $2^n$  mass functions to express the information under  $n$ -element frame of discernment (FoD), so the amount of data in BBA algorithm increases exponentially with increasing elements, which enables most of algorithms in DSET are NP problems.

<sup>★</sup>The work is partially supported by National Natural Science Foundation of China (Grant No. 61973332 and No. 61801459), JSPS Invitational Fellowships for Research in Japan (Short-term).

\*Corresponding author

✉ zhouqianli@std.uestc.edu.cn (Q. Zhou); tianguojing@ict.ac.cn (G. Tian); dengentropy@uestc.edu.cn (Y. Deng)

ORCID(s): 0000-0001-5087-3617 (Q. Zhou)

<sup>1</sup>This work was done when he was a research intern at ICT, CAS.

Facing the explosive growth of data is not only DSET, but many machine learning algorithms are also in this dilemma. The development of quantum computers is because Moore's Law is about to reach its limit, and scholars use the characteristics of quantum to process data more efficiently. Scholars begin to pay attention to the study of quantum computing because of the prime factor decomposition algorithm proposed by Shor (1999), which can solve the problem in polynomial time on quantum computer but in exponential time on classical computer. Another global search algorithm proposed by Grover can also achieve square-level acceleration on quantum computers (Grover (1996)). These algorithms prove that quantum computers have significant advantages over classical computers in certain problems, but due to the special requirements of quantum computing, quantum algorithms do not have much development in the field of machine learning. Until 2008, Giovannetti *et al.* proposed quantum random access memory (QRAM) and its implementation method (Giovannetti, Lloyd and Maccone (2008b) Giovannetti, Lloyd and Maccone (2008a), and in 2009, Harrow *et al.* proposed the HHL algorithm (Harrow, Hassidim and Lloyd (2009)), which used quantum algorithms to solve linear system problems (LSP). The above two works greatly promote the development of quantum machine learning (QML) (Biamonte, Wittek, Pancotti, Rebentrost, Wiebe and Lloyd (2017)). In recent years, more and more quantum machine learning algorithms have been proposed, such as quantum K-means cluster (Lloyd, Mohseni and Rebentrost (2013)), quantum Bayesian network (Low, Yoder and Chuang (2014)), quantum principle component analysis (QPCA) (Lloyd, Mohseni and Rebentrost (2014)), quantum neural networks (Altaisky (2001) Schuld, Sinayskiy and Petruccione (2014)) and so on. Compared with classical methods, quantum computer can store  $2^n$  data by superposition state under  $n$  qubits, and using reversible unitary operators to process the data in parallel.

In this paper, we encode BBA and belief functions under  $n$ -element FoD to superposition state under  $n$  qubits, and implement them on quantum circuit. In addition, we propose a new method called evidence fidelity to measure the similarity between BBAs and express it on quantum circuit. The contributions of the paper are summarized as follows: (1) BBA and belief function are encoded to quantum states called quantum basic belief assignment (QBBA) and quantum belief function, which makes qubits and elements have operational consistency. (2) According to QRAM (Giovannetti *et al.* (2008b)), an algorithm for implementation QBBA is proposed, which proves that extraction QBBA in QRAM can be exponentially accelerated compared to classic computers in running time. (3) The method of implement quantum belief functions is proposed and applied to the algorithm of plausibility transform method (Cobb and Shenoy (2006)), which also achieves exponential acceleration. (4) According to quantum fidelity (Nielsen and Chuang (2002)), a new method of inferring the similarity between BBAs called evidence fidelity is proposed, and proving that it can achieve the same decision-making effect as the evidence distance (Jousselme *et al.* (2001)) in classical. (5) The proposed evidence fidelity is expressed on quantum circuit based on the HHL algorithm (Harrow *et al.* (2009)) and swap test (Buhrman, Cleve, Watrous and De Wolf (2001)), which can measure the similarity between QBBA.

- (1) Section 2 introduce the preliminary knowledge required for the paper, including the basic concepts of evidence theory and quantum computation.
- (2) In Section 3, we propose the expression, preparation and extraction methods of QBBA and quantum belief function, and their implementation on the Qiskit platform. In addition, the advantages of quantum belief function is used to accelerate the plausibility transform method.
- (3) We first propose evidence fidelity in Section 4, which can rationally measure the similarity between BBAs, and propose the algorithm of measuring QBBA's similarity on quantum computer.
- (4) The Section 5 is a summary of full paper, describing our main contributions and existing unsolved problems.

## 2. Preliminaries

Some basic concepts of DSET and quantum computation are introduced in this section.

### 2.1. Dempster-Shafer evidence theory

As the generalization of probability theory, DSET can express more information.

**Definition 2.1 (BBA).** *Dempster (2008) For a finite element set  $\Theta = \{\theta_1, \dots, \theta_n\}$ , all mutually exclusive elements in  $\Theta$  form a closed space. The element in its power set  $2^\Theta = \{F_i\} = \{\{\emptyset\}, \{\theta_1\}, \dots, \{\theta_n\}, \{\theta_1\theta_2\}, \dots, \{\theta_1 \dots \theta_n\}\}$  is*

called focal element, which is composed by the elements in  $\Theta$ . The mass function  $m(F_i)$  is used to express the degree of support for elements in  $\{F_i\}$ , and they compose the basic belief assignment (BBA), where  $m(F_i)$  satisfies

$$m(F_i) \in [0, 1]; m(\emptyset) = 0; \sum_{F_i \in 2^\Theta} m(F_i) = 1. \quad (1)$$

The set  $\Theta$  is called frame of discernment (FoD), which corresponds to random variable in probability theory, and the element  $\theta_i$  corresponds to basic event.

Although BBA composed by mass functions can express the degree of support for focal elements, for the elements, it cannot reflect the uncertainty of them clearly. So the belief functions as the another expression of BBA are always used in decision-making.

**Definition 2.2 (Belief function).** *Shafer (1976)*

For a  $n$ -element FoD  $\Theta$  and BBA  $m(2^\Theta)$ , its belief (Bel) function, Plausibility (Pl) function and commonality ( $q$ ) function are defined as

$$Bel(F_i) = \sum_{G_i \subseteq F_i} m(G_i) = 1 - Pl(\overline{F_i}) \quad (2)$$

$$Pl(F_i) = \sum_{G_i \cap F_i \neq \emptyset} m(G_i) = 1 - Bel(\overline{F_i}) \quad (3)$$

$$q(F_i) = \sum_{F_i \subseteq G_i} m(G_i); \quad m(F_i) = \sum_{F_i \subseteq G_i} (-1)^{|G_i| - |F_i|} q(F_i) \quad (4)$$

where  $\overline{F_i}$  means the complement of  $F_i$ , and the Equ.4 is Mobius transformation. Bel function means the totally support degree to the focal element, and Pl function means the non-negation degree to the focal element, which compose the belief interval  $[Bel(F_i), Pl(F_i)]$ .

Because of mutual exclusion between elements, the focal element cannot be the result in decision-making. Transforming the BBA to probability distribution is an effective way to solve it. Cobb *et al.* propose the plausibility transformation method based on the Pl function, which is one of the widely applied method because of its consistency of Dempster combination rule.

**Definition 2.3 (PPF).** *Cobb and Shenoy (2006)* Given a BBA  $m(2^\Theta)$  under  $n$ -element FoD  $\Theta = \{\theta_1, \dots, \theta_n\}$ , the plausibility probability function (PPF) transformed by plausibility transformation method is defined as

$$Pl\_P(\theta_i) = \frac{Pl(\theta_i)}{\sum_{i=1}^n Pl(\theta_i)}, \quad (5)$$

where  $Pl(\theta_i)$  is the plausibility function of  $\theta_i$ . The time complexity of plausibility transformation method under  $n$ -element FoD is  $\mathcal{O}(n2^{n-1} + n)$ , which is composed with the solve plausibility function  $\mathcal{O}(n2^{n-1})$  and normalization them  $\mathcal{O}(n)$ .

In the process of handling information, for different evidences obtained from different sources, a reasonable measurement of the differences between them is significant. Since focal elements are not completely mutually exclusive, Euclidean distance cannot accurately measure the difference of evidences. So in DSET, the most commonly used method is the evidence distance proposed by Jousselme *et al.*.

**Definition 2.4 (Evidences distance).** *Jousselme et al. (2001)* For a  $n$ -element FoD, suppose two BBAs from different sources are  $m_1(2^\Theta)$  and  $m_2(2^\Theta)$ , and the evidence distance between them is defined as

$$d_{BBA}(m_1, m_2) = \sqrt{\frac{1}{2}(\vec{m}_1 - \vec{m}_2)^T \underline{\underline{D_E}}(\vec{m}_1 - \vec{m}_2)}, \quad (6)$$

where  $\vec{m}$  is the vector of mass function, and  $\underline{\underline{D_E}}$  is an  $2^n \times 2^n$  matrix whose elements  $\underline{\underline{D_E}}(F_i, G_i) = \frac{|F_i \cap G_i|}{|F_i \cup G_i|}$ .

Jousselme *et al.* utilize a coefficient matrix  $\underline{\underline{D_E}}$  to express the similarity between different focal elements. In this way, focal elements that are not completely mutually exclusive can be processed reasonably, so the evidence distance can objectively describe the difference between different evidences. Since the value range of evidence distance is  $d_{BBA} \in [0, 1]$ , Deng *et al.* Yong, Wenkang, Zhenfu and Qi (2004) utilize  $1 - d_{BBA}(m_1, m_2)$  to describe the degree of similarity between the BBAs  $m_1$  and  $m_2$ .

## 2.2. Quantum computation

### 2.2.1. Qubit

In classical information theory, bit is elementary unit of information, whose state is either 0 or 1. In quantum computing Nielsen and Chuang (2002), qubit is the elementary unit of quantum information, which exists in the form of superposition in the calculation process. The Dirac notations are usually used to describe the state in quantum. Any quantum state orthogonal to each other can be used as the basis states of calculations. Commonly the ket  $|0\rangle$  and  $|1\rangle$  are used as the basis, whose representation and superposition  $|\Psi\rangle$  are expressed as follows:

$$|0\rangle = \begin{bmatrix} 1 \\ 0 \end{bmatrix}; |1\rangle = \begin{bmatrix} 0 \\ 1 \end{bmatrix}; |\Psi\rangle = c_1 |0\rangle + c_2 |1\rangle = \begin{bmatrix} c_1 \\ c_2 \end{bmatrix}, \quad (7)$$

where  $c_1$  and  $c_2$  are complex number and satisfy  $|c_1|^2 + |c_2|^2 = 1$ .  $|c_i|^2$  means the probability amplitude of the state  $|i\rangle$  after measurement. When there are multiple qubits, the tensor product  $\otimes$  can form a new superposition state. Suppose two states  $|\Psi_1\rangle = c_1 |0\rangle + c_2 |1\rangle$  and  $|\Psi_2\rangle = d_1 |0\rangle + d_2 |1\rangle$ , their joint state  $|\Psi_1\rangle \otimes |\Psi_2\rangle = c_1 d_1 |00\rangle + c_1 d_2 |01\rangle + c_2 d_1 |10\rangle + c_2 d_2 |11\rangle$ .

For a qubit in a pure state, it can be described as a point on the Bloch sphere Nielsen and Chuang (2002). By rotating  $\phi$  around the  $y$ -axis and rotating  $\theta$  around the  $z$ -axis, its amplitude and phase can be determined respectively. So given parameter  $(\phi, \theta)$ , any qubit can be written as  $|\Psi\rangle = \cos(\frac{\theta}{2}) |0\rangle + e^{i\phi} \sin(\frac{\theta}{2}) |1\rangle$ . For the mixed state, it is a point in the Bloch sphere, which is usually represented by a density matrix. Suppose in a quantum system, there are quantum state  $|\Psi_i\rangle$  with the probability  $p_i$ , and the density matrix of it can be represented as  $\rho = \sum_i p_i |\Psi_i\rangle \langle \Psi_i|$ .

### 2.2.2. Quantum gates

Different from classical computing, the process of quantum computing is the unitary transformation of quantum states,  $|\Psi_1\rangle = U |\Psi_0\rangle$ , which also determines that quantum computing is reversible. For the quantum state formed by  $n$  qubits, the operator performing the unitary transformation is a  $2^n \times 2^n$  unitary matrix. which acts on the quantum state in the form of a quantum gate on the quantum circuit. Table 1 shows several common basic gates in quantum algorithms and their matrix representations. It can be seen from Nielsen and Chuang (2002) that Y-Rotation gate, Z-Rotation gate, and CNOT gate can form a general basic gate library, i.e., any unitary transformation can be realized by using only these three gates.

In this section, we introduce the basic concepts of evidence theory and quantum computing. For common quantum algorithms, we will introduce them later when they are used. If you need a deeper understanding of quantum computing, please refer to Nielsen and Chuang (2002).

## 3. Quantum Dempster-Shafer evidence theory

It can be seen from the above that in quantum computing,  $n$  qubits can express  $2^n$  data, and the  $n$  elements in the DSET also correspond to  $2^n$  focal elements. According to the method of expressing focal elements with binary codes proposed in Smets (2002), we correspondingly encode classical BBA to the quantum state.

**Table 1**

(1)Pauli-X gate is to reverses the state, i.e.  $X|0\rangle \rightarrow |1\rangle$ . (2)Y-Rotation gate is to rotate the state  $\theta$  around the y-axis, which changes the amplitude of the state. (3)Z-Rotation gate is to rotate the state  $\lambda$  around the z-axis, which is equivalent to adding a global phase to the  $|1\rangle$  and maintaining the  $|0\rangle$ . (4)Hadamard gate is one of the most useful gates. It can transform  $|0\rangle$  and  $|1\rangle$  into their intermediate states  $|+\rangle = \frac{1}{\sqrt{2}}(|0\rangle + |1\rangle)$  and  $|-\rangle = \frac{1}{\sqrt{2}}(|0\rangle - |1\rangle)$  respectively, and it also satisfies  $HH^\dagger = I$ . (5)For any single-bit gate, it can be decomposed into two Z-Rotation gates and one Y-Rotation gate. i.e. Three parameters  $(\phi, \lambda, \theta)$  can determine a unique unitary matrix. (6)The CNOT gate is composed of the control bit  $c$  and the target bit  $t$ . When the control bit is  $|1\rangle$ , the target bit is reversed (using the Pauli-X gate). There may be more than one control bit called  $C^n - NOT$  gate, which can entangle multiple qubits.

Quantum Gates	Pauli-X gate	Y-Rotation gate	Z-Rotation gate	Hadamard gate	Single-bit gate	CNOT gate
Notation						
Matrix	$\begin{bmatrix} 0 & 1 \\ 1 & 0 \end{bmatrix}$	$\begin{bmatrix} \cos(\frac{\theta}{2}) & \sin(\frac{\theta}{2}) \\ -\sin(\frac{\theta}{2}) & \cos(\frac{\theta}{2}) \end{bmatrix}$	$\begin{bmatrix} 1 & 0 \\ 0 & e^{i\lambda} \end{bmatrix}$	$\frac{1}{\sqrt{2}} \begin{bmatrix} 1 & 1 \\ 1 & -1 \end{bmatrix}$	$\begin{bmatrix} \cos(\frac{\theta}{2}) & -e^{i\lambda} \sin(\frac{\theta}{2}) \\ e^{i\phi} \sin(\frac{\theta}{2}) & e^{i(\phi+\lambda)} \cos(\frac{\theta}{2}) \end{bmatrix}$	$\begin{bmatrix} 1 & 0 & 0 & 0 \\ 0 & 1 & 0 & 0 \\ 0 & 0 & 0 & 1 \\ 0 & 0 & 1 & 0 \end{bmatrix}$

**Table 2**

Each qubit corresponds to an element. When the quantum state is  $|1\rangle$ , the corresponding element exists in the focal element. When the qubit is  $|0\rangle$ , the intersection of the corresponding element and the focal element is empty.

Quantum state	$ 0\rangle^{\otimes n}$	$ 0\rangle^{\otimes n-1} 1\rangle$	$ 0\rangle^{\otimes n-1} 1\rangle 0\rangle$	...	$ 0\rangle^{\otimes n-2} 1\rangle^{\otimes 2}$	...	$ 1\rangle^{\otimes n}$
Focal element	$\{\emptyset\}$	$\{\theta_1\}$	$\{\theta_2\}$	...	$\{\theta_1\theta_2\}$	...	$\{\theta_1 \dots \theta_n\}$

### 3.1. Quantum basic belief assignment

**Definition 3.1 (QBBA).** For a  $n$ -element FoD  $\Theta$  and its power set  $2^\Theta = \{F_i\} = \{\{\emptyset\}, \{\theta_1\}, \dots, \{\theta_n\}, \{\theta_1\theta_2\}, \dots, \{\theta_1 \dots \theta_n\}\}$ ,  $n$  qubits can be expanded into focal elements of the power set according to Table 2.

the quantum basic belief assignment (QBBA)  $\Psi_m$  is defined as follows:

$$\Psi_{m(2^\Theta)} = \sum_{j=1}^{2^n} \sqrt{m(F_j)} |j\rangle = \sqrt{m(\theta_1)} |0\dots 01\rangle + \sqrt{m(\theta_2)} |0\dots 10\rangle + \dots + \sqrt{m(\theta_1 \dots \theta_n)} |1\dots 11\rangle \quad (8)$$

Where the square of the state amplitude is equal to the mass function of the corresponding focal element.

How to accurately implement classical data on a quantum computer is an open issue. QBBA stores the mass function directly on the amplitude, so we use QRAM to extract the QBBA proposed by Giovannetti Giovannetti et al. (2008b) Giovannetti et al. (2008a). Prakash proposed a tree-like memory structure in his PhD thesis Prakash (2014), which can store classical information, but it can also be accessed in quantum superposition. Given a memory structure  $\mathbb{R}$  and an initial state  $|0\rangle^{\otimes n}$ , in order to implement an initial state  $|x\rangle$  containing  $2^n$  data, extract the data in  $\mathbb{R}$  to generate the required state  $|x\rangle = \sum_{i=1}^{2^n} x_i |i\rangle$ . The whole process can reach  $\mathcal{O}(n)$  in time with sufficient qubits, but in classical, it is  $\mathcal{O}(2^n)$ . In quantum circuit,  $\mathcal{O}(2^n)$  quantum gates are needed to complete the implementation. Based on the above, we propose a memory structure for storing QBBA, which is similar to the structure proposed by Dervovic Dervovic, Herbrster, Mountney, Severini, Usher and Wossnig (2018). The data stored by each node is equal to the sum of the data stored by their left and right child nodes. Combined with the special properties of QDSET, we can think that the root node represents the approximate state is  $|\tilde{1}\rangle^{\otimes n}$ , and their child nodes are the states  $|0\rangle$  and  $|1\rangle$  of qubit corresponding to an element. By analogy, for  $n$ -element FoD, only  $n$  layers are needed to store  $2^n$  mass functions. For a given access memory structure  $\mathbb{R}_m$ , the method of implement QBBA is shown in Algorithm 1.

**Algorithm 1** Implement QBBA from QRAM

**Input:** The BBA of  $n$ -element FoD,  $m(F_i)$ ,  $i = 1 : 2^n$ ; The tree-like memory structure,  $\mathbb{R}_m$ ;

**Output:** The state of quantum basic probability assignment,  $|x\rangle = \sum_{i=1}^{2^n} x_i |i\rangle$ ;

- 1: Prepare  $n$  qubits with initial state  $|x_0\rangle = |1\rangle^{\otimes n}$ , label them as  $q_0, \dots, q_n$ ;
- 2: Label the root node of the  $\mathbb{R}_m$  as  $u$  (the approximate state is  $|\tilde{1}\rangle^{\otimes n}$ );
- 3: **for** all parents nodes  $t$  in  $\mathbb{R}_m$  **do** execute  $\text{Calculate\_Node}(t)$ ;
- 4:    $\text{Calculate\_Node}(t)$  {
- 5:    $t_r$  and  $t_l$  respectively are the right and left child nodes of  $t$ , and rule the  $k$  is the layer of the  $t$  in the structure;
- 6:   The approximate state of  $t_r$  is the same as  $t$  and the  $k - th$  qubit in approximate state of  $t_r$  is reversed of  $t$ ;
- 7:    $\theta_i = \arccos(\sqrt{\frac{v(t_r)}{v(t)}}) = \arcsin(\sqrt{\frac{v(t_l)}{v(t)}})$ , where  $v(t)$  is the value of the node  $t$ ;
- 8:   Use  $R_y(2\theta_i)$  gate on  $t$ :  $|1\rangle_k \rightarrow -\sin(\theta) |0\rangle_{k+1} + \cos(\theta) |1\rangle_{k+1}$ ;
- 9:   }
- 10: **end for**
- 11: For the amplitude corresponding to the state of the bottom layer, the  $R_y(2\theta_i)$  gates on the same line are used on the  $|x_0\rangle$ . For example,  $|1\rangle^{\otimes n} = \prod_{\theta \text{ in a line}} \cos(\theta) |x_0\rangle$ ;
- 12: **return**  $|x_0\rangle$ ;

According to the Grover and Rudolph (2002), we also can implement the QBBA exactly on quantum circuit with controlled Y-Rotation gate. In order to facilitate understanding, we use Example 3.1 to introduce the implementation process of QBBA under 3-element FoD, which can be easily extended in the dimension of  $n$  elements.

**Example 3.1.** Given a BBA  $m = \{m(\emptyset), m(A), m(B), m(C), m(AB), m(AC), m(BC), m(ABC)\}$  under 3-element FoD  $X = \{A, B, C\}$ , the QRAM  $\mathbb{R}_m$  and the process of implementation QBBA based on Algorithm 1 are shown in Fig. 1.

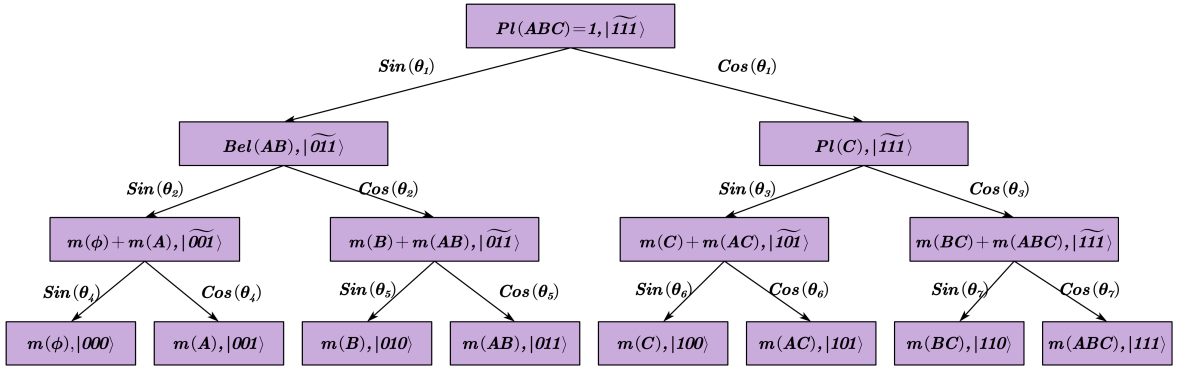


**Figure 1:** Since the special properties of BBA, the data generated in the process can also be represented by mass function and belief function, such as  $Bel(AB)$  and  $m(C) + m(AC)$ . Different QRAM construction methods can produce intermediate quantities with different meanings, so structure can be constructed according to the real need in computation, which is an advantages compared with the classical RAM.

The run time of 3-element FoD is  $\mathcal{O}(3)$ , and  $\mathcal{O}(7)$  gates can implement the QBBA on quantum circuits. After the operation in Fig. 2, the QBBA of  $X$  can be simulated in the state  $|\Psi_{m(2^X)}\rangle$ .

In summary, using QRAM can efficiently extract the classical BBA to quantum state.

## 3.2. Quantum belief function and its application

### 3.2.1. Quantum belief function

According to the Definition 2.2, belief functions can express the degree of support of one or some elements. Different from the mass functions of BBA, they emphasize the support degree in form of summation of mass functions. In the classical, to solve a belief function, the focal elements that meet the conditions need to be extracted from the



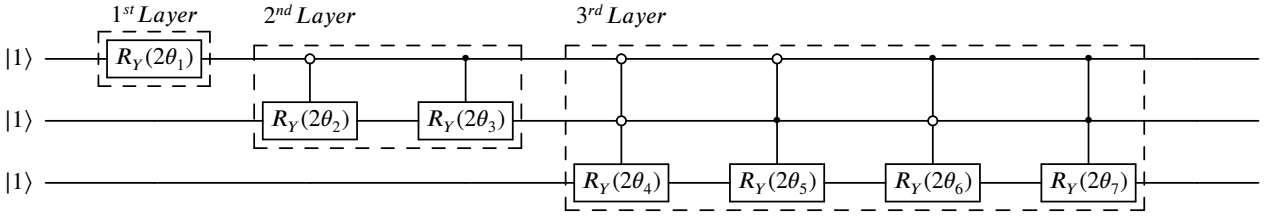


**Figure 2:** According to the structure in Figure 1, the controlled Y-Rotation gates can be used to simulate the evolution of each layer. To popularize this circuit, for  $n$ -element FoD, QBBA can be implemented with  $n$  qubits and  $2^n - 1$  quantum gates, and for the  $k$ -th layer,  $2^{k-1}$  gates are needed to simulate.

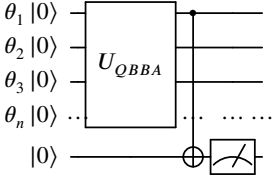


**Figure 3:**  
 $Pl(\theta_1) \& q(\theta_1) \& Bel(\theta_2 \dots \theta_n)$

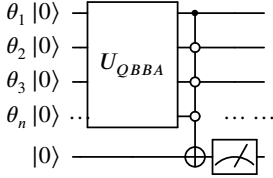


**Figure 4:**  
 $Bel(\theta_1) \& Pl(\theta_2 \dots \theta_n)$

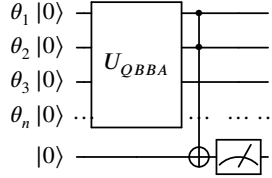


**Figure 5:**  
 $q(\theta_1 \theta_2)$

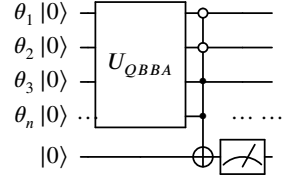


**Figure 6:**  
 $Bel(\theta_1 \theta_2) \& Pl(\theta_3 \dots \theta_n)$

BBA, and then they are summed. Suppose a belief function that requires  $k$  focal elements,  $\mathcal{O}(k)$  is required to calculate it. However, representing them utilizing the characteristic of qubit in quantum circuits only need one gate.

**Definition 3.2 (Quantum belief function).** Given a  $n$ -element FoD  $\Theta$  and its BBA  $m(2^\Theta)$ , the quantum belief (QBel) function  $|\Psi_{Bel(F_i)}\rangle$  and quantum plausibility (QPl) function  $|\Psi_{Pl(F_i)}\rangle$  are denoted as

$$\begin{aligned} |\Psi_{Bel(F_i)}\rangle &= \sqrt{Bel(F_i)} |1\rangle + \sqrt{Pl(\bar{F}_i)} |0\rangle; \\ |\Psi_{Pl(F_i)}\rangle &= \sqrt{Pl(F_i)} |1\rangle + \sqrt{Bel(\bar{F}_i)} |0\rangle \end{aligned} \quad (9)$$

where  $\bar{F}_i$  is the complement of  $F_i$  in  $\Theta$ . And the quantum commonality (Qq) function is denoted as

$$|\Psi_{q(F_i)}\rangle = \sqrt{q(F_i)} |1\rangle + \sqrt{1 - q(F_i)} |0\rangle \quad (10)$$

According to Equ. 9, we encode the belief function to an ancilla qubit, and a quantum state can express both belief function and plausibility function at the same time. In QBBA, extracting the amplitude of a certain qubit is equivalent to extracting its corresponding element's information in FoD. Therefore, for a prepared QBBA  $|\Psi_m\rangle$ , only one additional ancilla measurement qubit can extract arbitrary belief function and the process is  $|\Psi_m\rangle^n |0\rangle \rightarrow |\Psi_m\rangle^n (\sqrt{Pl} |1\rangle + \sqrt{Bel} |0\rangle)$ . Example 3.2 shows some belief functions implement on the quantum circuits.

**Example 3.2.** Given a  $n$ -element FoD  $\Theta$  and its BBA  $m(2^\Theta)$ , the QBBA can be implemented from a unitary operator  $U_{QBBA}$ . Fig.3-6 are the process of implement  $Pl(\theta_1) \& q(\theta_1) \& Bel(\theta_2 \dots \theta_n)$ ,  $Bel(\theta_1) \& Pl(\theta_2 \dots \theta_n)$ ,  $q(\theta_1 \theta_2)$  and  $Bel(\theta_1 \theta_2) \& Pl(\theta_3 \dots \theta_n)$  on quantum circuits.

It can be seen from Example 3.2 that using quantum circuits to implement the belief function has an acceleration effect compared to the classical method. Any belief function only needs a  $C^n NOT$  gate to implement a superposition state with its information. For quantum belief functions, their complexity optimization depends on the optimization of  $C^n NOT$  gates. The prepared quantum belief function can be used as a sub-algorithm in other algorithms. But extracting classical data from quantum state needs to perform a constant number of measurements.

### 3.2.2. Application of implementation quantum belief function: plausibility transformation method

Based on above, using  $C^n NOT$  gate can accelerate to implement the quantum belief function. Among them, for a  $n$ -element FoD, the most obvious acceleration effect is to solve  $Pl(\theta_i) \& q(\theta_i)$ . In classical, the time complexity of calculating  $Pl(\theta_i)$  requires  $\mathcal{O}(2^{n-1})$ , but only need 1 CNOT gate in QDSET algorithm, i.e. the quantum computation complexity is  $\mathcal{O}(1)$ . According to the Definition 2.3, the total algorithm is composed with two steps. For the first step, if we replace the solving PI function to implement quantum PI function and transform quantum function into classical data through constant number of measurements, the time complexity of solving PI function will be reduced to  $\mathcal{O}(n)$ .  $|\psi_m\rangle^n$  is the QBBA prepared according to Algorithm 1, and using  $n$  ancilla measurement qubits can implement the  $|\psi_{Pl(\theta_i)}\rangle$ .

$$|\psi_m\rangle^n |0\rangle^n \rightarrow |\psi_m\rangle^n (\sqrt{Pl(\theta_1)} |1\rangle + \sqrt{Bel(\theta_2 \dots \theta_n)} |0\rangle) \dots (\sqrt{Pl(\theta_n)} |1\rangle + \sqrt{Bel(\theta_1 \dots \theta_{n-1})} |0\rangle) \quad (11)$$

Add the time complexity of the second step, the total complexity of using quantum plausibility function to handle the plausibility transformation method is  $\mathcal{O}(n + n)$ , which obviously less than the classical complexity  $\mathcal{O}((n2^{n-1} + n))$ .

### 3.3. Simulation the QDSET using Qiskit

In order to prove the rationality of the proposed model, we simulated the implementation process of QBBA under 3-element FoD and the solution process of its belief functions on the Qiskit platform (IBM (2016). Ibm quantum experience. URL: <https://quantum-computing.ibm.com>) in Example 3.3.

**Example 3.3.** Given a BBA  $m(2^\Theta) = \{m(A) = \frac{1}{18}, m(B) = \frac{1}{6}, m(C) = \frac{1}{6}, m(AB) = \frac{1}{9}, m(AC) = \frac{1}{18}, m(BC) = \frac{4}{18}, m(ABC) = \frac{4}{18}\}$  under the FoD  $X = \{A, B, C\}$ , the  $Pl(C)$  and  $q(BC)$  is

$$\begin{aligned} Pl(C) &= m(C) + m(BC) + m(AC) + m(ABC) = \frac{5}{9} \\ q(BC) &= m(BC) + m(ABC) = \frac{4}{9} \end{aligned} \quad (12)$$

According to the Algorithm 1, we construct a quantum circuit to implement the QBBA  $|\Psi_{m(2^\Theta)}\rangle$  in Fig. 7. And the simulation result with 6172 shots shown in Fig. 8. The results of simulation prove that the information of DSET can be stored by quantum state and the slight error comes from the quantum itself.

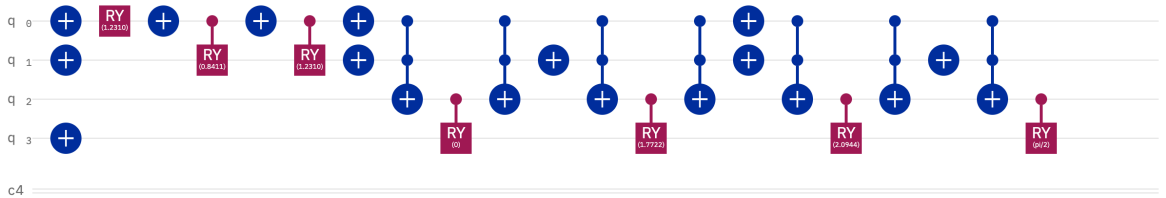


**Figure 7:** Based on the QRAM, use NOT gate, Y-Rotation gate, CNOT gate and CCNOT gate to implement the QBBA  $|\Psi_{m(X)}\rangle$ .

Since both quantum computation and DSET have power exponential property (i.e., using  $2^n$  data to describe  $n$  elements), using the characteristics of quantum computation can provide a new expression of DSET. In this section, we encode the BBA to quantum state and propose the quantum Dempster Shafer evidence theory (QDSET). First, the classic BBA is stored in a tree-like QRAM, and QBBA is implemented according to the structure by Y-Rotation operator. For the BBA under the  $n$ -element FoD, the complexity of extracting BBA data with the classic register is  $\mathcal{O}(2^n)$ , and the run time complexity in a quantum way is  $\mathcal{O}(n)$  (sufficient qubits), and  $\mathcal{O}(2^n)$  quantum gates are required to implement QBBA on a quantum circuit. Then we propose the implementation of quantum belief functions and prove its advantages over the classical. Finally, we simulated the above process on Qiskit to prove the rationality of our proposed model and algorithm.



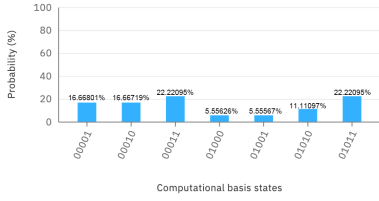


**Figure 8:** BBA is implemented on the amplitude of corresponding state.

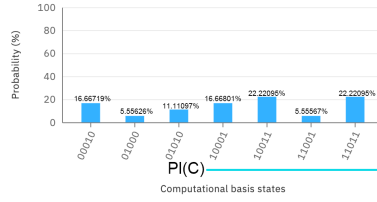


**Figure 9:** When the first bit is  $|1\rangle$ , the amplitude of the state is belong to  $Pl(C)$ .

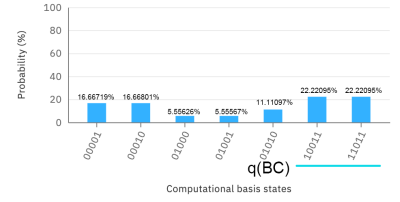


**Figure 10:** When the first bit is  $|1\rangle$ , the amplitude of the state is belong to  $q(BC)$ ,

## 4. Measure the similarity of QBAs

How to measure the similarities and differences between BBAs is an important issue in DSET. In addition to the evidence distance introduced in Definition 2.4, Xiao proposed the divergence measure of BBAs based on correlation coefficient Xiao (2019). The existing classical algorithms can infer the difference between BBAs reasonably, but their high complexity makes it difficult to directly apply them as measurement tools in practice. In quantum computation, there is no way to realize logarithmic operation for the time being, so Xiao's method cannot be used in QDSET. The evidence distance has subtraction operation, and addition and subtraction is not the acceleration advantage of quantum computation. In order to realize an algorithm can be implemented on quantum circuit with acceleration, we propose evidence fidelity to measure the similarity between BBAs, which can not only measure the similarity of BBAs rationally, but achieve an acceleration compared to the evidence distance in the classics as well. In addition, we propose corresponding quantum algorithm to realize the acceleration.

### 4.1. Evidence fidelity

In quantum computation, fidelity is well used in measure the similarity between states, whose computational properties have been verified in previous studies.

**Definition 4.1 (Quantum fidelity).** Nielsen and Chuang (2002) Given two quantum states in form of density matrix  $\rho$  and  $\sigma$ , the quantum fidelity of them is defined as

$$F(\rho, \sigma) = (\text{tr} \sqrt{\sqrt{\rho} \sigma \sqrt{\rho}}) \quad (13)$$

where  $\text{tr}(\cdot)$  is the trace of matrix. If the state is pure, which can be represented as  $\rho = |\phi\rangle\langle\phi|$  and  $\sigma = |\psi\rangle\langle\psi|$ , the fidelity of  $|\phi\rangle$  and  $|\psi\rangle$  can be written as  $F(|\phi\rangle, |\psi\rangle) = |\langle\psi|\phi\rangle|^2$ .

The value range of fidelity is  $[0, 1]$ . When two quantum states are more similar, the fidelity of them is closer to 1. If a quantum state measure the fidelity with itself, the result must be 1. In classical, it can be easily extend to measure the similarity of probability distributions.

**Definition 4.2 (Probability fidelity).** Nielsen and Chuang (2002) Given two  $n$ -dimensional probability distribution  $\vec{p} = \{p_1, \dots, p_n\}$  and  $\vec{q} = \{q_1, \dots, q_n\}$ , define the  $\sqrt{\vec{p}} = \{\sqrt{p_1}, \dots, \sqrt{p_n}\}$ . So the fidelity between  $\vec{p}$  and  $\vec{q}$  is defined as

$$F(\vec{p}, \vec{q}) = \sum_{i=1}^n \sqrt{p_i q_i} = \sqrt{p_1 q_1} + \sqrt{p_2 q_2} + \sqrt{p_3 q_3} + \dots + \sqrt{p_n q_n}. \quad (14)$$

The physical meaning of fidelity is the inner product of  $\sqrt{\vec{p}}$  and  $\sqrt{\vec{q}}$  on the sphere, so it is reasonable to use it to measure the similarity between probability distributions. For DSET, before using fidelity for two BBAs, the original BBA must be processed, because unlike the complete mutual exclusion of basic events in probability theory, focal elements are not completely mutually exclusive. Jousselme et al. use a coefficient matrix to express the relation of different focal elements, but it can not be used in BBA directly. So we propose a new method to handle the original BBA Zhou and Deng (2020), which can solve the problem rationally. Based on above, the fidelity of evidence in classical has been solved.

**Definition 4.3 (Evidence fidelity).** Given two BBAs  $m_1$  and  $m_2$  under  $n$ -element FoD, the evidence fidelity of them is defined as

$$F(\vec{m}_1, \vec{m}_2) = \sum_{i=1}^{2^n} \sqrt{\vec{m}_1^F(F_i) \vec{m}_2^F(F_i)} \quad (15)$$

where  $\sqrt{\vec{m}^F}$  is denoted as

$$\sqrt{\vec{m}^F(F_i)} = \sqrt{\frac{m(F_i)}{2^{|F_i|} - 1}} + \sum_{F_j \subset G_i \text{ and } F_j \neq G_i} \sqrt{\frac{m(G_j)}{2^{|G_j|} - 1}}. \quad (16)$$

The operation of Equ. 16 is equivalent to applying an invertible upper triangular matrix  $\underline{FB}$  to  $\sqrt{\vec{m}}$ , and it can be written as

$$\begin{array}{ccccccc} & \{\emptyset\} & \{\theta_1\} & \dots & \{\theta_n\} & \{\theta_1\theta_2\} & \dots & \{\theta_1 \dots \theta_n\} \\ \{\emptyset\} & 1 & 0 & \dots & 0 & 0 & \dots & 0 \\ \{\theta_1\} & 0 & 1 & \dots & 0 & \frac{1}{\sqrt{3}} & \dots & \frac{1}{\sqrt{2^{|\{\theta_1 \dots \theta_n\}|} - 1}} \\ \vdots & \vdots & \vdots & \ddots & \vdots & \vdots & \ddots & \vdots \\ \{\theta_n\} & 0 & 0 & \dots & 1 & 0 & \dots & \frac{1}{\sqrt{2^{|\{\theta_1 \dots \theta_n\}|} - 1}} \\ \{\theta_1\theta_2\} & 0 & 0 & \dots & 0 & \frac{1}{\sqrt{3}} & \dots & \frac{1}{\sqrt{2^{|\{\theta_1 \dots \theta_n\}|} - 1}} \\ \vdots & \vdots & \vdots & \ddots & \vdots & \vdots & \ddots & \vdots \\ \{\theta_1 \dots \theta_n\} & 0 & 0 & \dots & 0 & 0 & \dots & \frac{1}{\sqrt{2^{|\{\theta_1 \dots \theta_n\}|} - 1}} \end{array} \quad (17)$$

so the  $\sqrt{\vec{m}^F}$  also can be written as  $\sqrt{\vec{m}^F} = \underline{FB} \times \sqrt{\vec{m}}$ .

In order to prove the rationality and necessity of evidence fidelity, we compare it with evidence distance and probability fidelity in Example4.1. Based on this, it can be seen that both evidence fidelity and evidence distance can measure the similarity of evidence in a reasonable way, but probability fidelity produces undesirable results in some situations since it does not consider the relationship between focal elements.

**Example 4.1.** Given two BBAs  $m_1$  and  $m_2$  of a 2-element FoD  $X = \{A, B\}$ , two cases of their distributions are shown as follows:

$$\begin{aligned} \text{Case1 : } m_1(A) &= \frac{1-a}{2}; m_1(B) = a; m_1(AB) = \frac{1-a}{2} \\ m_2(A) &= 0; m_2(B) = \frac{1}{2}; m_2(AB) = \frac{1}{2} \\ \text{Case2 : } m_1(A) &= 0; m_1(B) = \frac{1}{5} + b; m_1(AB) = \frac{4}{5} - b \\ m_2(A) &= 1; m_2(B) = 0; m_2(AB) = 0. \end{aligned} \quad (18)$$

When the  $a : 0 \rightarrow 0.5$  and  $b : 0 \rightarrow 0.8$ , the change trend of evidence distance, evidence fidelity and probability fidelity are shown in Fig. 11.

In Example 4.2, a pattern recognition example based on Dempster combination rules shows the satisfactory effect of evidence fidelity.

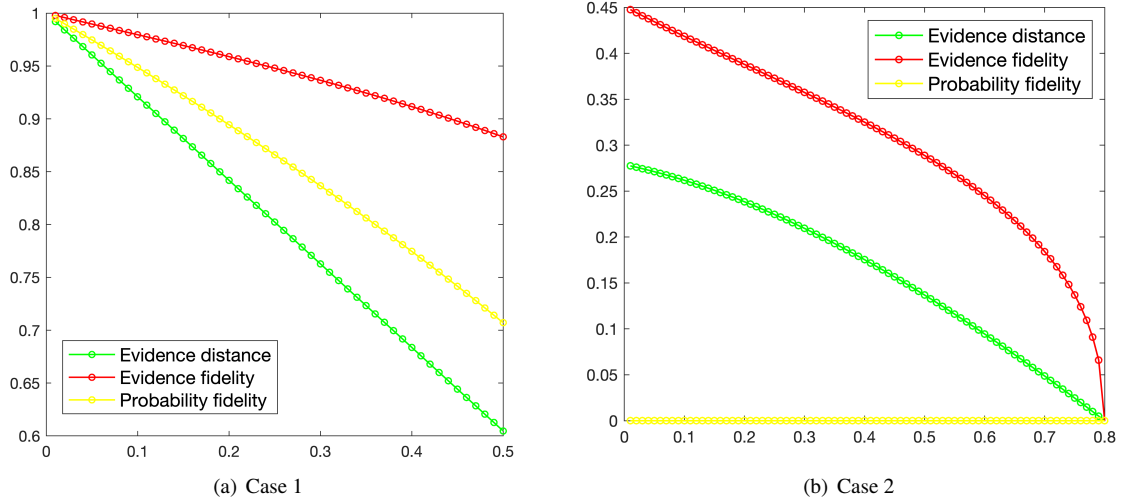


**Figure 11:** In order to ensure the similarity of changing trends, we use  $1 - d_{BBA}$  to represent the similarity between the evidences. In order to satisfy the realization in quantum computing, we normalized  $\sqrt{m^F}$  before calculating fidelity to ensure that its 2-norm equal to 1. (a) Case 1 proved that when the BBA changes uniformly, three methods can effectively measure their similarity. (b) When a situation similar to Case 2, probability fidelity cannot measure their similarity, because although the focal elements are completely different, the elements are still related.

**Table 3**

The recognition result after information fusion indicates that the evidence fidelity can not only identify the objective correctly, but realize better fusion results than previous.

Methods	{A}	{B}	{C}	{AC}	Target
DempsterDempster (2008)	0.0000	0.1422	0.8578	0.0000	C
MurphyMurphy (2000)	0.9620	0.0210	0.0138	0.0032	A
Deng et al.Yong et al. (2004)	0.9820	0.0034	0.0115	0.0032	A
XiaoXiao (2019)	0.9905	0.0002	0.0072	0.0039	A
Evidence fidelity	0.9945	0.0011	0.0020	0.0005	A

**Example 4.2.** Suppose three objectives represented by a 3-element FoD  $X = \{A, B, C\}$ , 5 sensors  $\{S_1, S_2, S_3, S_4, S_5\}$  receive different information about the objectives:

$$\begin{aligned}
 S_1 : m_1(A) &= 0.41; m_1(B) = 0.29; m_1(C) = 0.30; m_1(AC) = 0.00 \\
 S_2 : m_2(A) &= 0.01; m_2(B) = 0.90; m_2(C) = 0.10; m_2(AC) = 0.00 \\
 S_3 : m_3(A) &= 0.58; m_3(B) = 0.07; m_3(C) = 0.00; m_3(AC) = 0.35 \\
 S_4 : m_4(A) &= 0.55; m_4(B) = 0.10; m_4(C) = 0.00; m_4(AC) = 0.35 \\
 S_5 : m_5(A) &= 0.60; m_5(B) = 0.10; m_5(C) = 0.00; m_5(AC) = 0.30.
 \end{aligned} \tag{19}$$

We utilize the algorithm proposed in Yong et al. (2004) to eliminate distractions and identify the right target, and the final result of target recognition is shown in the Table 4.

#### 4.2. Measure the similarity of QBAs: Quantum evidence fidelity

Based on the Section 3, the QBA can be exactly implemented in a quantum state on quantum circuit. We propose an algorithm based on HHL algorithms Harrow et al. (2009) and swap test Buhrman et al. (2001) to measure the evidence fidelity between QBAs on quantum circuit. According to the classic evidence fidelity, the quantum evidence fidelity algorithm can be divided into two steps. The first step is to apply matrix  $\underline{FB}$  to QBA, and the second step is to solve the fidelity of these two evolved QBAs. For the first step, we arrive the evolved QBA based on HHL algorithm. HHL algorithm Harrow et al. (2009) is proposed in 2009 to solve linear system problem on quantum circuit,

whose appearance has attracted widespread attention and promoted the development of quantum machine learning. For the problem of solving linear equation  $Ax = b$ , the quantum state  $|b\rangle$  containing the information of the vector  $\vec{b}$  and a reversible Hermitian matrix  $\underline{A}$  are input into the HHL algorithm, and the output is the normalized target vector  $|x\rangle$ . The output vector is a quantum state, its properties can only be used as a sub-algorithm, and its value cannot be obtained concretely, but it is enough to solve many problems. The detailed algorithm principle is introduced in Dervovic et al. (2018). In addition, 2-dimensional and 4-dimensional vectors are implemented on quantum circuits in Cao, Daskin, Frankel and Kais (2012) and Schleich (2019). Its classical complexity are  $\mathcal{O}(N^3)$  in Gauss elimination and  $\mathcal{O}(Nsk \log \frac{1}{\epsilon})$  in conjugate gradient algorithm for sparse, and the HHL can reduce to  $\mathcal{O}(\kappa^2/\epsilon s^2 \log N)$ . Since the HHL algorithm only has an acceleration effect on sparse Hermitian matrix.<sup>2</sup>  $\underline{FB}$  is neither a sparse matrix nor a Hermitian matrix, so it cannot be directly applied to quantum circuits. We first decompose  $\underline{FB}$  through singular value decomposition (SVD) to obtain unitary matrices  $\underline{U}_S$  and  $\underline{U}_V$  and diagonal matrix  $\underline{D}$ . Unitary operators can be directly implemented on quantum circuits. Based on the HHL algorithm, the diagonal matrix can also be used on QBBA. So the entire  $\underline{FB}$  evolves on QBBA. The swap test uses two Hadamard gates and one swap gate to obtain the fidelity of any two quantum states, which has been widely used in algorithms in recent years. Next, the algorithm for solving the fidelity of quantum evidence will be introduced from two parts the evolution of QBBA and solving the fidelity.

#### 4.2.1. The evolution of QBBA

We perform SVD of matrix  $\underline{FB}_n$  (evolved matrix under  $n$ -element FoD) into  $\underline{FB}_n = \underline{U}_S \underline{D} \underline{U}_V$ , where  $\underline{U}_S$  and  $\underline{U}_V$  are unitary matrices, and  $\underline{D}$  is a diagonal matrix. First, we apply the  $\underline{U}_V$  operator to QBBA,

$$|\psi_m\rangle = \sum_{i=0}^{2^n-1} \sqrt{m(i)} |i\rangle \xrightarrow{\underline{U}_V} \sum_{i=0}^{2^n-1} \sqrt{m^V(i)} |i\rangle = |\psi_m^V\rangle. \quad (20)$$

Then, we proposed an evolutionary algorithm based on HHL to apply  $\underline{D}$  on  $|\psi_m^V\rangle \rightarrow |\psi_m^D\rangle$ . Finally use the unitary operator  $\underline{U}_S$  to get the target state  $|\psi_m^F\rangle$ . Based on above, the core step is the evolutionary algorithm, which is composed of three steps: phase estimation, controlled rotation and uncomputation.

##### Step1: Phase estimation

The spectral decomposition of  $\underline{D}$  is  $\underline{D} = \sum_{j=0}^{2^n-1} \lambda_j |c_j\rangle \langle c_j|$ , and the  $\lambda_j$  and  $|c_j\rangle$  are eigenvalues and eigenvectors. According to  $e^{i\underline{D}t} |c_j\rangle = e^{i\lambda_j t} |c_j\rangle$ , the eigenvectors of  $\underline{D}$  can be represented in the phase of a the state  $|c_j\rangle$ . In the phase estimation algorithm Cleve, Ekert, Macchiavello and Mosca (1998) Luis and Peřina (1996), the eigenvector of matrix  $\underline{D}$  needs to be used.

$$|\psi_m^V\rangle = \sum_{i=0}^{2^n-1} \sqrt{m^V(i)} |i\rangle = \sum_{j=0}^{2^n-1} \alpha_j |c_j\rangle \langle c_j|j\rangle = \sum_j \beta_j |c_j\rangle \quad (21)$$

According to the phase estimation in Fig. 12, two quantum registers are needed in this step, one register  $T$  is used to represent the  $|\psi_m^V\rangle$  and another called clock register can simulate the time of evolution. After phase estimation, the eigenvalues of matrix  $\underline{D}$  with  $2^n$  precisions are stored in the clock register.

$$U_P : |0\rangle^N |\psi_m^V\rangle = \sum_j |0\rangle^N \beta_j |c_j\rangle \rightarrow \sum_{j,t} \epsilon_{j,t} \beta_j |\tilde{\lambda}_j\rangle |c_j\rangle \quad (22)$$

The  $\epsilon_{j,t}$  is a constant produced in the estimation process.  $|\tilde{\lambda}_j\rangle$  is the result that the target eigenvalues is represented by an  $N$ -bit binary number. In the rest algorithm, we assume that it is accurate, so it is recorded as  $|\lambda_j\rangle$ . In this step, we draw the eigenvectors of  $\underline{D}$  to the quantum state from phase and change the basis of the  $|\psi_m^V\rangle$ .

<sup>2</sup>Sparse matrix: For an  $N$ -dimensional matrix, the number of non-zero elements in each row or column does not exceed  $\log N$  at most.

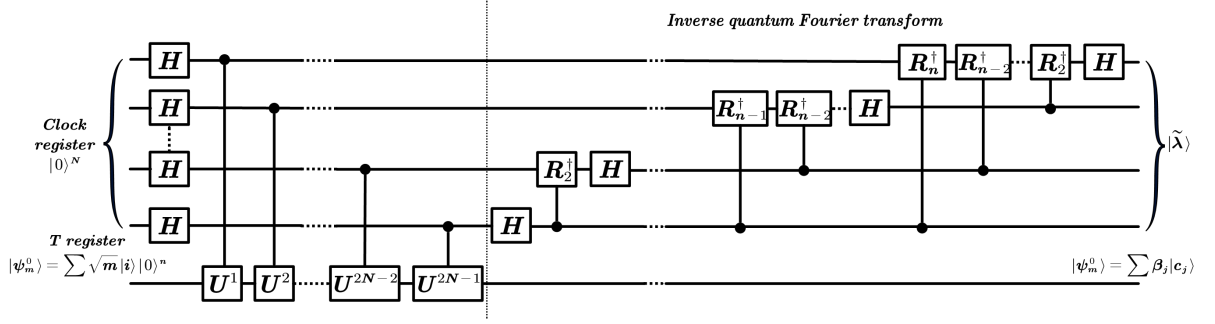


**Figure 12:** The clock register is to simulate the evolution of time, apply the desired phase to the superposition state, and then use the inverse quantum Fourier transform (the specific process of quantum Fourier transform can refer to Nielsen and Chuang (2002)) to obtain a binary representation of the phase with a precision of  $N$ . The T register is entangled with Clock register by controlled-U gate, where  $U = \exp(-i\mathbf{D}t)$ , and the output is itself with the eigenvector of  $\mathbf{D}$  as the orthogonal basis.

### Step2: Controlled rotation

The ultimate goal is to calculate the state containing the information of  $\mathbf{D}|\psi_m^V\rangle$ . Because of  $\mathbf{D}\beta_j|c_j\rangle = \lambda_j\beta_j|c_j\rangle$ ,  $\lambda_j$  in state  $|\lambda_j\rangle$  needs to be extracted to act on  $\sum_j \beta_j|c_j\rangle$ . Assume that  $\tilde{\theta}$  is the representation of  $\theta$  with binary precision of  $d$ , it must be existing unitary  $U_{\theta} = \sum_{\theta \in \{0,1\}^d} |\tilde{\theta}\rangle \langle \tilde{\theta}| \otimes \exp(-i\tilde{\theta}\sigma_y) = R_y(\tilde{\theta})$  gate satisfies that

$$U_{\theta} : |\tilde{\theta}\rangle |0\rangle \rightarrow |\tilde{\theta}\rangle (\cos(\tilde{\theta}) |0\rangle + \sin(\tilde{\theta}) |1\rangle). \quad (23)$$

So the third ancilla qubit is needed to represent the  $\lambda_j$ , and according to the Equ.23, following the result in Step1, the  $U_{\theta}$  can achieve

$$\sum_j |0\rangle |\lambda_j\rangle \beta_j |c_j\rangle \rightarrow \sum_j (\sqrt{1 - K^2 \lambda_j^2} |0\rangle + K \lambda_j |1\rangle) |\lambda_j\rangle \beta_j |c_j\rangle, \quad (24)$$

where  $K$  is normalization coefficient, and  $\theta = \arccos(K\lambda_j)$ .

### Step3: Uncomputation

After the above two steps of operation, the three quantum registers have been entangled together. Our goal is to determine whether the state in  $T$  is the result we need by measuring the state of ancilla qubit, so the state of clock register will interfere with our measurement results, whose state is  $|0\rangle^N$  after inverse operation of first step. The uncomputation is also called resolving the entanglement.

$$U_P^\dagger : \sum_j (\sqrt{1 - K^2 \lambda_j^2} |0\rangle + K \lambda_j |1\rangle) |\lambda_j\rangle \beta_j |c_j\rangle \rightarrow \sum_j (\sqrt{1 - K^2 \lambda_j^2} |0\rangle + K \lambda_j |1\rangle) |0\rangle \beta_j |c_j\rangle \quad (25)$$

Then measure the ancilla qubit whether equals to 1, i.e., project on  $|1\rangle$ -subspace.

$$|1\rangle \langle 1| : \sum_j \beta_j (\sqrt{1 - K^2 \lambda_j^2} \langle 1|0\rangle + K \lambda_j \langle 1|1\rangle) |1\rangle |0\rangle |c_j\rangle \quad (26)$$

So when the ancilla qubit is  $|1\rangle$ , the target state is in the T register:

$$|\psi_m^D\rangle = \frac{1}{\sqrt{\sum_j K^2 \beta_j^2 \lambda_j^2}} \sum_j K \beta_j \lambda_j |c_j\rangle = \frac{\mathbf{D}|\psi_m^V\rangle}{\|\mathbf{D}|\psi_m^V\rangle\|} \quad (27)$$

The whole process of evolution of BBA is similar with HHL algorithm, the more detail can refer Harrow et al. (2009) Dervovic et al. (2018).

#### 4.2.2. Swap test

For the evolved QBBA, we do not need to obtain its specific value through multiple measurements before calculating the fidelity. The swap test proposed in Buhrman et al. (2001) can directly put the fidelity of the two quantum states into the amplitude of the ancilla bit. For two evolved QBBA's  $|\psi_{m_1}^F\rangle$  and  $|\psi_{m_2}^F\rangle$  with a ancilla qubit, the process is shown as follows:

$$\begin{aligned} |0\rangle |\psi_{m_1}^F\rangle |\psi_{m_2}^F\rangle &\xrightarrow{H \otimes I \otimes I} \frac{1}{\sqrt{2}}(|0\rangle + |1\rangle) |\psi_{m_1}^F\rangle |\psi_{m_2}^F\rangle \xrightarrow{c-SWAP} \frac{1}{\sqrt{2}} |0\rangle |\psi_{m_1}^F\rangle |\psi_{m_2}^F\rangle + \frac{1}{\sqrt{2}} |1\rangle |\psi_{m_2}^F\rangle |\psi_{m_1}^F\rangle \\ &\xrightarrow{H \otimes I \otimes I} \frac{1}{2} |0\rangle (|\psi_{m_1}^F\rangle |\psi_{m_2}^F\rangle + |\psi_{m_2}^F\rangle |\psi_{m_1}^F\rangle) + \frac{1}{2} |1\rangle (|\psi_{m_1}^F\rangle |\psi_{m_2}^F\rangle - |\psi_{m_2}^F\rangle |\psi_{m_1}^F\rangle) \xrightarrow{P(|1\rangle)} \frac{1}{2} - \frac{1}{2} |\langle \psi_{m_1}^F | \psi_{m_2}^F \rangle|^2. \end{aligned} \quad (28)$$

Therefore, the fidelity of the two states can be obtained by performing a constant number of measurements on the ancilla bit. The above evolution is simulated in the case of an ideal quantum computer. And the total circuits of measuring the similarity of quantum evidence is shown in Fig13.

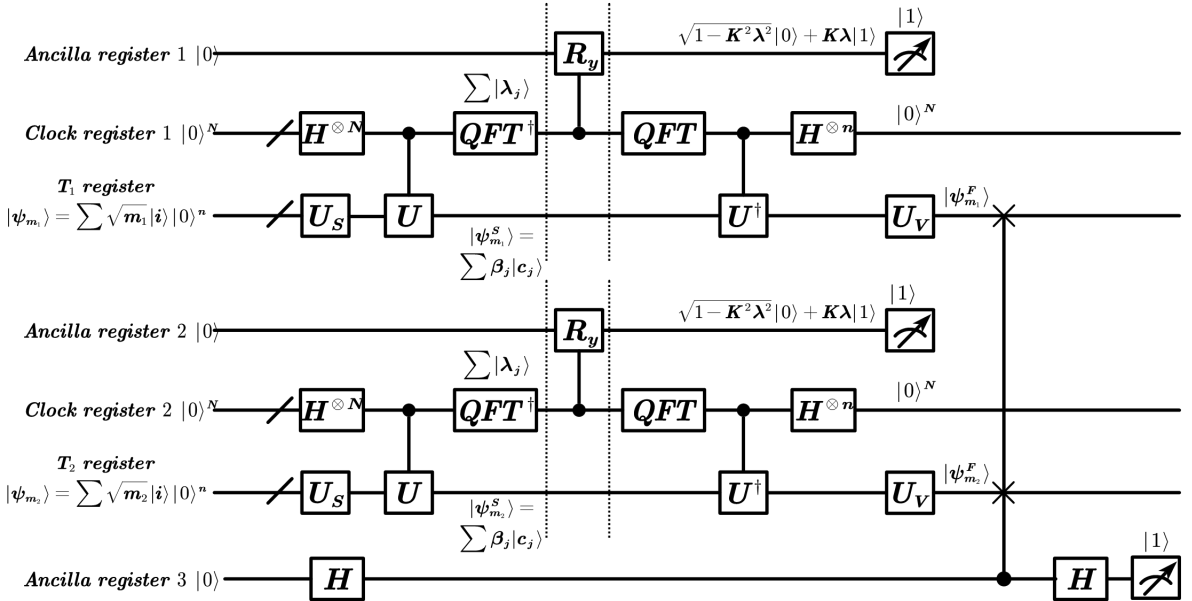


**Figure 13:** Algorithm schematic of measuring the similarity between QBBA's: The whole algorithm have two steps. (a) According to the introduction in 4.2.1, through the three processes of phase estimation, controlled rotation, and uncomputation, when the measurement result of ancilla register 1 & 2 is  $|1\rangle$ , the  $T$  register at this time is the evolved QBBA. (b) Pass the state of the registers  $T_1$  and  $T_2$  through the swap test, and measure the probability of the ancilla bit 3 being  $|1\rangle$  to get the similarity of the original QBBA's. It is worth noting that the results of the three ancilla bits at this time should all be  $|1\rangle$ .

### 4.3. Complexity analysis

In order to prove the superiority of using quantum evidence fidelity, we analyze the complexity of the three algorithms quantum evidence fidelity, evidence distance and evidence fidelity respectively. The steps of these three methods can be summarized into two steps. One step is to infer the difference between the two evidences, and the other step is to process the focal element relationship by applying the matrix to the vector. For a  $n$ -element FoD, we represent its complexity with  $n$ , so the number of focal elements is  $2^n - 1$ .



**Table 4**  
Complexity

Methods	Matrix operation	Difference inference
Evidence distance	$\mathcal{O}(2^n \cdot (2^n - \frac{3^n}{2}) + 2^{n+1})$	$\mathcal{O}(2^n)$
Evidence fidelity	$\mathcal{O}(2^{n+1}((\frac{3}{2})^n - 1) + 2^n)$	$\mathcal{O}(2^{n+1})$
Quantum evidence fidelity	$\mathcal{O}(n\sqrt{2^n - 1/\epsilon} + S_n + V_n)$	$\mathcal{O}(n)$

**Evidence distance** The first step in solving the evidence distance is to subtract two BBA vectors, and the required complexity is  $\mathcal{O}(2^n)$ . The non-zero entries of  $\underline{D_E}$  is the sum of the number of  $PI(F_i)$  under FoD.

$$\sum_{i=1}^n \binom{n}{i} (2^n - 2^{n-i}) = 2^n (2^n - (\frac{3}{2})^n) \quad (29)$$

So, the complexity of matrix operation can be calculated in  $\mathcal{O}(2^{n+1}(2^n - (\frac{3}{2})^n) + 2^{n+1})$ .

**Evidence fidelity** The step of matrix operation is evolution the BBA by  $\underline{FB}$ , and the non-zero entries of  $\underline{FB}$  is the sum of the number of  $q(F_i)$  under FoD.

$$\sum_{i=1}^n \binom{n}{i} 2^{n-i} = 2^n (\frac{3}{2})^n - 1 \quad (30)$$

So, the complexity of matrix operation can be calculated in  $\mathcal{O}(2^{n+1}((\frac{3}{2})^n - 1) + 2^n)$ . And the complexity of inferring difference step is  $\mathcal{O}(2^{n+1})$

**Quantum evidence fidelity** Measure the fidelity of QBBA's under  $n$ -element FoD only need  $n$  controlled SWAP gates, so swap test to infer difference between QBBA's can realize exponential acceleration. Based on the Dervovic et al. (2018), the flow of QBBA evolution algorithm is similar with HHL algorithm without amplitude amplification, and the complexity of HHL is  $\mathcal{O}(\kappa^2/\epsilon s^2 \log N)$ , where  $s$  is sparse degree of the matrix,  $\kappa$  is the ratio of the maximum absolute eigenvalue to the minimum absolute eigenvalue and  $\epsilon$  is the error produced in phase estimation. For the QBBA evolution algorithm, the sparse degree is 1, and the  $\kappa$  is  $\sqrt{2^n - 1}$ , and the amplitude amplification need  $\mathcal{O}(\kappa)$ . So the complexity of evolution algorithm is  $\mathcal{O}(n\sqrt{2^n - 1/\epsilon})$ . In addition, there are two unitary operators  $\underline{U_S}$  and  $\underline{U_V}$  in whole evolution process, and the costs of implementation them is  $\mathcal{O}(S_n)$  and  $\mathcal{O}(V_n)$ .

Based on the above analysis, we show the complexity of the three algorithms in Table 4. Although the application of quantum algorithms in the evolution process and the infer difference are accelerated exponentially, for the complexity of the overall algorithm, the number of basic gates that generate the two unitary operators  $\underline{U_S}$  and  $\underline{U_V}$  needs to be considered. According to the Shende, Bullock and Markov (2006), precise implementation of arbitrary unitary operators requires high complexity  $\mathcal{O}(\frac{23}{48}4^n)$ , which makes the entire quantum algorithm lose its acceleration effect. In Cross, Bishop, Sheldon, Nation and Gambetta (2019), an approximate method of preparing a unitary operator is proposed. For quantum circuits below 4 qubits, the authors have verified that it is possible to prepare arbitrary unitary operators with a complexity  $\mathcal{O}(2^n)$  with error rate of 5%.

## 5. Conclusion

In order to solve the problem of the power exponential explosion of DSET algorithms on classical computers, this paper proposes QDSET and proves that its algorithms can be significantly accelerated on quantum computers. Even if the quantum states are orthogonal, this cannot correspond to the incompletely mutually exclusive focal elements in a physical sense, we can use the characteristics of quantum computing to speed up the solution of problems in classical evidence theory.

The characteristic of quantum computation is  $n$  qubits can represent  $2^n$  data at the same time, which is consistent with utilizing  $2^n$  mass functions to describe  $n$  elements in DSET. We encode the BBA to the quantum state, which

allows qubits to directly control the corresponding elements' mass functions. In classical, for multi-element FoD, the order of mass functions is often considered when dealing with BBA. However, in quantum computation, the qubits operation is equivalent to directly changing the belief functions, which makes the DSET has great application prospects in quantum computation. We propose a method of extracting QBBA based on QRAM. When the number of qubits is large enough, the preparation of QBBA can be exponentially accelerated in time and the quantum belief functions of QBBA can be arrived by a  $C^n - NOT$  gate directly. We verified the rationality of QDSET on the Qiskit platform and applied this acceleration effect to the plausibility transformation method. In summary, we establish the basic model of DSET under quantum computation, which proves that the handling BBA on the quantum computer has exponential acceleration, and provides a new research direction for the algorithm of DSET.

Evidence fidelity based on quantum fidelity and fractal-based matrix is proposed in the paper. we prove the necessity of fractal-based matrix and show it can achieve the similar effect on difference inference of BBAs with evidence distance. The new proposed method can not only reduce the complexity in classical, but be implemented on quantum circuit as well. Quantum evidence fidelity is proposed based on HHL algorithm and swap test. After complexity analysis, under ideal low-dimensional conditions, quantum evidence fidelity can achieve exponential acceleration compared to classics. Quantum evidence fidelity shows that the relationship between focal elements can still be handled on quantum circuits, which ensures the universality of DSET algorithms in quantum computation.

For the future, this paper has some issues worthy of study. (1) Although the tree-like structure QRAM can accelerate the implementation of QBBA, based on existing research, the less number of qubits is equally important in quantum computation. Proposing a preparation method that can use fewer qubits and has low time complexity can make it more valuable in practical applications. (2) The different rules of quantum algorithms and classical algorithms result in that not all algorithms can be accelerated on quantum computers, so it is important to choose a reasonable DSET algorithm or convert the classical DSET algorithm into an algorithm that can be accelerated on a quantum computer. (3) we assume that the SVD decomposition has been completed, which is also an ideal situation. How to integrate the QSVD algorithm with the existing algorithm, and reduce the complexity of high-dimensional Hamiltonian simulation, is significant for quantum evidence fidelity algorithm.

## Bibliography

## References

- Altaisky, M., 2001. Quantum neural network. arXiv preprint quant-ph/0107012 .
- Biamonte, J., Wittek, P., Pancotti, N., Rebentrost, P., Wiebe, N., Lloyd, S., 2017. Quantum machine learning. *Nature* 549, 195–202.
- Buhrman, H., Cleve, R., Watrous, J., De Wolf, R., 2001. Quantum fingerprinting. *Physical Review Letters* 87, 167902.
- Cao, Y., Daskin, A., Frankel, S., Kais, S., 2012. Quantum circuit design for solving linear systems of equations. *Molecular Physics* 110, 1675–1680.
- Cleve, R., Ekert, A., Macchiavello, C., Mosca, M., 1998. Quantum algorithms revisited. *Proceedings of the Royal Society of London. Series A: Mathematical, Physical and Engineering Sciences* 454, 339–354.
- Cobb, B.R., Shenoy, P.P., 2006. On the plausibility transformation method for translating belief function models to probability models. *International journal of approximate reasoning* 41, 314–330.
- Cross, A.W., Bishop, L.S., Sheldon, S., Nation, P.D., Gambetta, J.M., 2019. Validating quantum computers using randomized model circuits. *Physical Review A* 100, 032328.
- Dempster, A.P., 2008. Upper and lower probabilities induced by a multivalued mapping, in: *Classic works of the Dempster-Shafer theory of belief functions*. Springer, pp. 57–72.
- Deng, X., Zheng, X., Su, X., Chan, F.T., Hu, Y., Sadiq, R., Deng, Y., 2014. An evidential game theory framework in multi-criteria decision making process. *Applied Mathematics and Computation* 244, 783–793.
- Denoeux, T., 1994. Application of evidence theory to k-nn pattern classification, in: *Machine Intelligence and Pattern Recognition*. Elsevier, volume 16, pp. 13–24.
- Dervovic, D., Herbster, M., Mountney, P., Severini, S., Usher, N., Wossnig, L., 2018. Quantum linear systems algorithms: a primer. arXiv preprint arXiv:1802.08227 .
- Dezert, J., Tchamova, A., Han, D., 2018. Total belief theorem and conditional belief functions. *International Journal of Intelligent Systems* 33, 2314–2340.
- Giovannetti, V., Lloyd, S., Maccone, L., 2008a. Architectures for a quantum random access memory. *Physical Review A* 78, 052310.
- Giovannetti, V., Lloyd, S., Maccone, L., 2008b. Quantum random access memory. *Physical review letters* 100, 160501.
- Grover, L., Rudolph, T., 2002. Creating superpositions that correspond to efficiently integrable probability distributions. arXiv preprint quant-ph/0208112 .
- Grover, L.K., 1996. A fast quantum mechanical algorithm for database search, in: *Proceedings of the twenty-eighth annual ACM symposium on Theory of computing*, pp. 212–219.
- Harrow, A.W., Hassidim, A., Lloyd, S., 2009. Quantum algorithm for linear systems of equations. *Physical review letters* 103, 150502.
- Jousselme, A.L., Grenier, D., Bossé, É., 2001. A new distance between two bodies of evidence. *Information fusion* 2, 91–101.

- Lloyd, S., Mohseni, M., Rebentrost, P., 2013. Quantum algorithms for supervised and unsupervised machine learning. arXiv preprint arXiv:1307.0411 .
- Lloyd, S., Mohseni, M., Rebentrost, P., 2014. Quantum principal component analysis. Nature Physics 10, 631–633.
- Low, G.H., Yoder, T.J., Chuang, I.L., 2014. Quantum inference on bayesian networks. Physical Review A 89, 062315.
- Luis, A., Peřina, J., 1996. Optimum phase-shift estimation and the quantum description of the phase difference. Physical review A 54, 4564.
- Murphy, C.K., 2000. Combining belief functions when evidence conflicts. Decision support systems 29, 1–9.
- Nielsen, M.A., Chuang, I., 2002. Quantum computation and quantum information.
- Prakash, A., 2014. Quantum algorithms for linear algebra and machine learning. Ph.D. thesis. UC Berkeley.
- Schleich, P., 2019. How to solve a linear system of equations using a quantum computer .
- Schuld, M., Sinayskiy, I., Petruccione, F., 2014. The quest for a quantum neural network. Quantum Information Processing 13, 2567–2586.
- Shafer, G., 1976. A mathematical theory of evidence. volume 42. Princeton university press.
- Shende, V.V., Bullock, S.S., Markov, I.L., 2006. Synthesis of quantum-logic circuits. IEEE Transactions on Computer-Aided Design of Integrated Circuits and Systems 25, 1000–1010.
- Shor, P.W., 1999. Polynomial-time algorithms for prime factorization and discrete logarithms on a quantum computer. SIAM review 41, 303–332.
- Smets, P., 2002. The application of the matrix calculus to belief functions. International Journal of Approximate Reasoning 31, 1–30.
- Xiao, F., 2019. Multi-sensor data fusion based on the belief divergence measure of evidences and the belief entropy. Information Fusion 46, 23–32.
- Yaghlane, B.B., Smets, P., Mellouli, K., 2002. Belief function independence: Ii. the conditional case. International Journal of Approximate Reasoning 31, 31–75.
- Yong, D., Wenkang, S., Zhenfu, Z., Qi, L., 2004. Combining belief functions based on distance of evidence. Decision support systems 38, 489–493.
- Zhou, Q., Deng, Y., 2020. Fractal-based belief entropy. arXiv preprint arXiv:2012.00235 .
- Zhou, Q., Mo, H., Deng, Y., 2020. A new divergence measure of pythagorean fuzzy sets based on belief function and its application in medical diagnosis. Mathematics 8, 142.